Closed Formulas for Tunneling Time in Superlattices

Pedro Pereyra
Departamento de Ciencias Básicas, UAM-Azcapotzalco CP 02200, México Distrito Federal, México
(Received 5 May 1999)

New formulas for an exact and simple evaluation of the phase time associated with the passage of electrons or photons through a finite superlattice are derived. This time, named here the superlattice-tunneling time τ_n, exhibits a resonant-band structure or a superluminal phase time behavior depending on whether the particle's energy lies in a band or a gap. In the band, τ_n remains larger than the free motion time τ_f, while in the gap it can be less than τ_f (with strong substrate effects), but it is larger than the single-cell phase time τ_1. Extremely good agreements with optical-pulse and superluminal delay times measured by Spielmann *et al.* and Steinberg *et al.* are found, including the superlattice-tunneling-time limit and the substrate effects. Conditions for measurements of earlier electron arrival are also analyzed.

PACS numbers: 73.40.Gk, 42.50.Dv, 78.66.–w, 78.20.Ci

In the last several years enlightening and accurate measurements of single-photon and optical-pulse delay times, in the photonic band gap of multilayer media [1,2], have stimulated interest and controversy on the elusive concept of tunneling time. Earlier evanescent electromagnetic-wave experiments [3–5], new "tunneling time" definitions [6–9], and review papers [10,11] contributed significantly to maturing the discussion on this subject. Even though the debate on the tunneling time remains, the single-photon superluminal tunneling reported by Steinberg *et al.* [1] upholds the belief that tunneling time is well described by the "phase time" defined [12,13] as the frequency derivative of the transmission amplitude's phase θ_t. Spielman *et al.* [2] reported other evidences on superluminal delay times with appealing indications of the existence of a tunneling-time limit, that would be reached by increasing the number of cells in the superlattice (see Fig. 1). An important characteristic of this classical two-pulse interference experiment is the negligible distortion of wave packets in a broad photonic band gap. Their theoretical calculations (open triangles in Fig. 1) are, however, remarkably different from the measured delay times.

If we write the phase time as

$$\tau = |t|^{-2}(t_r \partial t_i/\partial\omega - t_i \partial t_r/\partial\omega), \qquad (1)$$

where t_r and t_i are the real and imaginary parts of the transmission amplitude t, it is clear that very accurate experimental measurements and very precise transmission-amplitude calculations are required to verify τ when a particle's energy lies in the gap where the transmission coefficient tends to zero. In the absence of analytic and rigorous evaluations, numerical or approximated theoretical calculations obscure this subtle and controversial issue. In this Letter, I show that the phase time associated with the passage (tunneling or no tunneling) of electrons or photons through a finite superlattice is a relevant quantity, which I calculate explicitly and compare with existing experimental data and denote it as the superlattice-tunneling (or transmission) time (STT) τ_n.

The transmitted wave packet's distortion is a consequence rather than a mechanism of the tunneling (or transmission) time behavior as a function of the energy $E = \hbar\omega$. In the transfer matrix approach to the passage of wave packets through a 1D scattering region extending from z_a to z_b, the transmitted wave packet at (z, τ) with $z \geq z_b$ and $\tau \geq \tau_b$ is given by

$$\psi_t(z,\tau) = \int A_k |t(k)| e^{i[kz - k(z_b - z_a) + \theta_t(k) - \omega\tau]}\, dk\,, \qquad (2)$$

where $t(k) = |t(k)|e^{i\theta_t(k)}$ is the k-component transmission amplitude and $\tau = \tau_b - \tau_a = \partial\theta_t(k)/\partial\omega$ is its phase time. Different k components have different phase times and transmission probabilities. The wave packet reshaping results then, basically, from these energy dependences.

In a superlattice, the phase interference phenomena determine strongly the energy behavior of the scattering

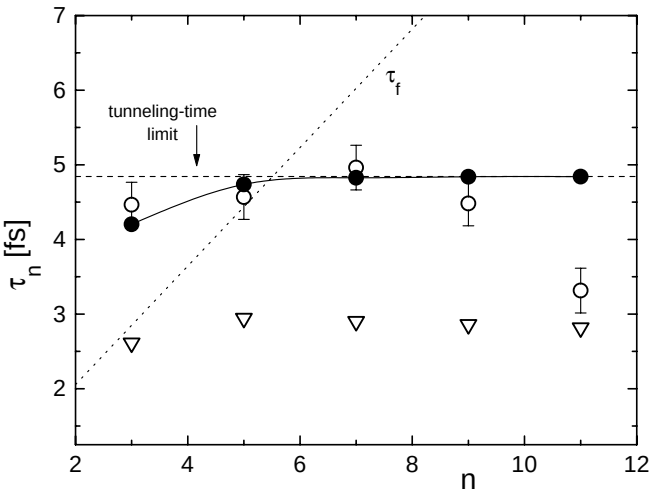

FIG. 1. Calculated and measured optical-pulse tunneling time τ_n through $(\lambda/4)$ superlattice $L(HL)^n$ with different values of n. The calculated times of the present work (full circles) are compared with those measured and calculated by Spielmann *et al.* (open circles and open triangles, respectively). The free motion time τ_f and the tunneling-time limit τ_∞ are also shown.

 0031-9007/00/84(8)/1772(4)$15.00

amplitudes. New and rigorous formulas, obtained recently [14] in the theory of finite periodic systems, are crucial to deduce analytic expressions for the scattering-amplitude phases and, hence, for the superlattice phase times τ_n of massive and nonmassive particles. Applying these times to the previously mentioned experimental cases, extremely good agreement is found with the experimental delay time measurements (see Fig. 1), and interesting energy-dependent properties, including the STT limit, emerge. Optimum conditions for massive particle superlattice-tunneling time measurements are also discussed below.

If we have a superlattice, say $(AB)^n$, the single-cell (AB) transfer matrix M (assuming time-reversal invariance) has the general structure

$$M = \begin{pmatrix} \alpha & \beta \\ \beta^* & \alpha^* \end{pmatrix}, \tag{3}$$

and the transmission amplitude t_n through the whole superlattice $(AB)^n$ is given by [14]

$$t_n = \frac{t^*}{t^* p_n - p_{n-1}}, \tag{4}$$

where $t\ [= t_r + i t_i = (\alpha^*)^{-1}]$ is the single-cell transmission amplitude and $p_n(\alpha_r)$ is the Chebyshev polynomial of order n evaluated at the real part of α $(= \alpha_r + i\alpha_i)$. All the information on the fundamental and intricate phase interference phenomena is carried out by these polynomials, to which order is related the superlattice size $l = nl_c$ (with l_c the unit-cell length). Given the transmission amplitude, a straightforward calculation leads to the *superlattice-tunneling (or transmission) time*

$$\tau_n = \frac{\hbar}{(p_n - \alpha_r p_{n-1})^2 + (\alpha_i p_{n-1})^2} \times \left(A_r \frac{d\alpha_r}{dE} + A_i \frac{d\alpha_i}{dE} \right), \tag{5}$$

with

$$A_r = \frac{\alpha_i}{1 - \alpha_r^2} [(\alpha_r p_{n-1} + n p_{n-2}) p_n - (n + \alpha_r^2) p_{n-1}^2], \tag{6}$$

and

$$A_i = (p_n - \alpha_r p_{n-1}) p_{n-1}. \tag{7}$$

To evaluate this time, all we need is the single-cell transfer matrix element α and its energy derivative. If more than one propagating mode is present, t is a matrix and we will have different phase times τ_{ij} strongly modified by channels mixing [14,15].

Before applying Eq. (5) to evaluate massive and nonmassive particle's phase times through specific systems, let us briefly mention the stunning optical-pulse STT limit, which occurs as the number of cells increases and a gap is built. This and Hartmann's prediction [16] are related properties but not exactly the same thing. The experimental behavior in Ref. [2] leads us naturally to ask whether a limit as $n \to \infty$ exists for τ_n. The answer is yes. After doing a little algebra we obtain

$$\tau_\infty \simeq \frac{\tau_1}{1 - T} + \frac{T}{1 - T} \left[\frac{\alpha_i}{2(1 - \alpha_r^2)} \frac{d\alpha_r}{dE} - \frac{1}{2\alpha_r} \frac{d\alpha_i}{dE} \right], \tag{8}$$

where τ_1 and T are the single-cell tunneling time and transmission probability, respectively. It is worth noticing that $\tau_n \sim \tau_\infty$ already for n of the order of 10 (see, for example, Figs. 1 and 2 where this occurs for $n = 8$), while the transmission probability approaches zero. For typical semiconductor superlattices the single-cell electron transmission probability T in the low energy gaps is close to zero, thus $\tau_\infty \sim \tau_1 \sim 10^{-13}$ s. On the other hand, optical $\lambda/4$ superlattices are characterized by a wide low-frequency gap where T is close to 1, and hence $\tau_\infty > \tau_1 \sim 1$ fs. Equations (5) and (8) are the main results of this Letter. Their predictions, shown below, agree well with the experimental results.

In order to illustrate the use of the previous formulas, two types of systems will be considered: a mass particle moving through a superlattice $A(BA)^n$ made of GaAs (A) and $Al_xGa_{1-x}As$ (B) and photons moving through dielectric mirrors. In the latter case we shall consider the $\lambda/4$ superlattices $(HL)^n H(substrate L)$ and $L(HL)^n$ made of titanium oxide (H) and silica (L) layers as in Refs. [1] and [2], respectively.

We shall start calculating the electron STT through the superlattice $(A^{1/2}BA^{1/2})^n$ contained between two GaAs thick layers. In this case, Eq. (5) can be directly applied. All we need is the single-cell $A^{1/2}BA^{1/2}$ transfer matrix or just its well-known matrix element

$$\alpha = e^{ikd_A} \left(\cosh\kappa d_B + i \frac{k^2 - \kappa^2}{2k\kappa} \sinh\kappa d_B \right), \tag{9}$$

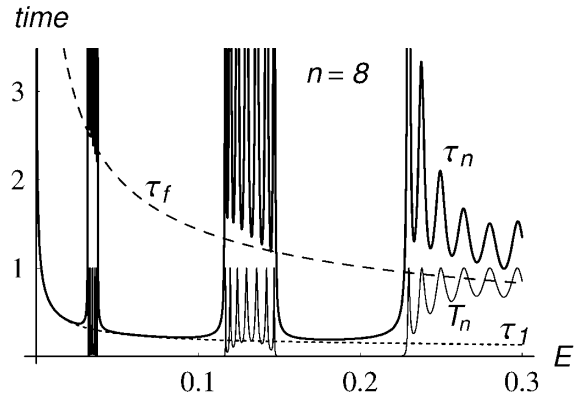

FIG. 2. The electron tunneling time τ_n (heavy line) follows the resonant behavior of dimensionless transmission probability T_n (light line) as a function of the energy (in eV). In this figure the superlattice $(Al_{0.3}Ga_{0.7}As/GaAs)^n$ parameters are used (see text). In the allowed energy band τ_n is larger than the free motion time τ_f (dashed curve), while in the gaps $\tau_n < \tau_f$ but is larger than the single-cell tunneling time τ_1 (dotted curve).

where

$$k = \sqrt{\frac{2m_A^*}{\hbar^2}\,E}\,, \quad \text{and} \quad \kappa = \sqrt{\frac{2m_B^*}{\hbar^2}\,(V_o - E)}\,. \tag{10}$$

Some relevant physical quantities are plotted in Fig. 2 for $V_0 = 0.23$ eV, electron effective masses $m_B^* = 0.1m_e$ and $m_A^* = 0.067m_e$, and barrier and valley widths $d_B = 3$ nm and $d_A = 10$ nm. In this figure, times are given in units of 10^{-13} s. The free motion time $\tau_f = nl_c m_e/\hbar k$ and the single-barrier phase time τ_1 are shown together with the transmission coefficient $T_n = |t_n|^2$ and the STT τ_n, for $n = 8$. A band structure is apparent for both the transmission coefficient T_n and the time τ_n. In the gaps, T_n tends to zero and τ_n approaches τ_1, which behaves as a lower bound. In the band region, on the other hand, the STT exhibits a resonant behavior whose lower bound is the free motion time τ_f. Up to this point, it is clear that the particle's dwelling time in the scatterer region grows as its energy approaches any allowed energy level. On the contrary, in the forbidden energy regions the particle runs away faster, reflecting the evanescent behavior and the lack of hospitality in the potential region.

To measure earlier electron arrival times, a two barrier structure [i.e., the heterostructure $substrate A(BA)^n$ with $n = 2$] might be an appropriate system. Although the difference $\tau_f - \tau_2$ is slightly less than $\tau_f - \tau_n$ (for $n \geq 3$), the transmission probability T_2 is much larger than T_n. On the other hand, for fixed barrier height and width, τ_2 and the subband level density increase with d_A while T_2 diminishes. If we choose $d_B = 3$ nm and $d_A = 15$ nm for $Al_xGa_{1-x}As$ and GaAs, respectively, and the remaining parameters are as mentioned before, earlier arrival times of about 20 fs and transmission coefficients of the order of 3% are predicted for incoming electron energies around $E \simeq 110$ meV (see Fig. 3). In the presence of an electric force F, the STT behavior of Fig. 3 remains almost equal, except for some important effects for energies between $V_0 - F(d_s + 2d_B + d_A)$ and $V_0 - F(d_s + d_B)$ and an origin displacement by approximately d_sF (assuming ballistic motion and substrate width d_s).

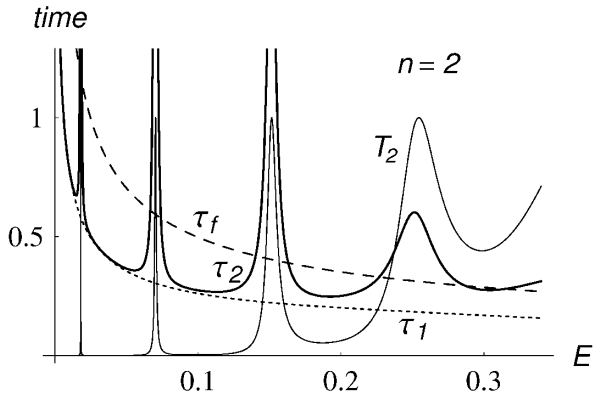

FIG. 3. Two barrier electron tunneling time τ_2 (heavy line) plotted together with the dimensionless transmission probability T_2 (light line), through the $GaAs(Al_{0.3}Ga_{0.7}As/GaAs)^2$ heterostructure, and the free motion time τ_f (dashed curve) as functions of the incident-particle energy (in eV).

Concerning the transmission of photons studied in Ref. [1], some care has to be taken since photons move from air to the dielectric mirror and again to air. To deal with the system of Ref. [1] one has to include the coupling transfer matrices

$$M_{aH} = \frac{1}{2n_H}\begin{pmatrix} e^{ik_H l_L} & 0 \\ 0 & e^{-ik_H l_L} \end{pmatrix}\begin{pmatrix} 1 + n_H & 1 - n_H \\ 1 - n_H & 1 + n_H \end{pmatrix},$$

and $M_{Ha} = M_{L_s a}M_{HL_s}$. Here

$$M_{HL_s} = \frac{1}{2n_L}\begin{pmatrix} n_H + n_L & n_H - n_L \\ n_H - n_L & n_H + n_L \end{pmatrix}\begin{pmatrix} e^{ik_H l_R} & 0 \\ 0 & e^{-ik_H l_R} \end{pmatrix},$$

and $M_{L_s a}$ is similar to M_{HL_s} but with l_R, n_H, and n_L replaced by l_s(the substrate's width), n_L, and 1, respectively. $l_{L(R)}$ is the left(right) H-layer width, $n_L = 1.41$ and $n_H = 2.22$ are the refractive indices, and $k_i = \omega n_i/c$ $(i = H, L)$. The whole system's $H_{l_L}(H^{1/2}LH^{1/2})^n H_{l_R}L_s$ transfer matrix is then

$$\tilde{M}_n = M_{Ha}M_nM_{aH} = M_{Ha}\begin{pmatrix} \alpha_n & \beta_n \\ \beta_n^* & \alpha_n^* \end{pmatrix}M_{aH} \tag{11}$$

$$= \begin{pmatrix} \tilde{\alpha}_n & \tilde{\beta}_n \\ \tilde{\beta}_n^* & \tilde{\alpha}_n^* \end{pmatrix}, \tag{12}$$

where M_n is the superlattice transfer matrix with elements [15]

$$\begin{aligned} \alpha_n &= p_n - \alpha^* p_{n-1}\,, \\ \beta_n &= \beta p_{n-1}\,. \end{aligned} \tag{13}$$

As mentioned before, α and β are the single-cell transfer matrix elements and p_n the Chebyshev polynomial evaluated at the real part of α [see Eq. (3)]. Although the modified transfer matrix element $\tilde{\alpha}_n$ $(= \tilde{\alpha}_{nr} + i\tilde{\alpha}_{ni})$ differs from α_n, it is still a simple function of the same Chebyshev polynomials p_n. In the particular case of Ref. [1], the single-cell transfer matrix elements (for normal incidence) are the well-known functions

$$\begin{aligned} \alpha &= \frac{e^{ik_H d_H}}{4n_H n_L}\left[e^{ik_L d_L}(n_H + n_L)^2 - e^{-ik_L d_L}(n_H - n_L)^2\right], \\ \beta &= i\,\frac{n_H^2 - n_L^2}{2n_H n_L}\sin k_L d_L = i\beta_i\,. \end{aligned} \tag{14}$$

Using the parameter values corresponding to the superlattice mirror $(HL)^n H$ of Ref. [1] with $l_s = \lambda/2$, we obtain the STT behavior shown in Fig. 4. As in Eq. (5), the only frequency derivatives that one has to evaluate are those of the single-cell functions α_r and α_i. The STT is an extremely sensitive quantity to the substrate-layer width l_s. To show this we plot (see Fig. 5) τ_f and $\tilde{\tau}_n$ as functions of l_s. For $l_s = m\lambda/4$ (with m even) $\tilde{\tau}_n < \tau_f$, while for odd multiples $\tilde{\tau}_n > \tau_f$. Intermediate values are of course possible. The transmission coefficient $\tilde{T}_n$ and the time $\tilde{\tau}_n$, for $n = 5$, shown in Fig. 4, again exhibit a resonant behavior.

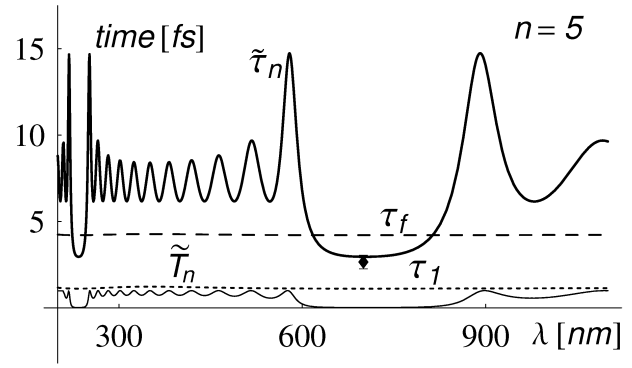

FIG. 4. Electromagnetic plane wave tunneling time $\tilde{\tau}_n$ (heavy line) and dimensionless transmission probability $\tilde{T}_n$ (light line) through the $(\lambda/4)$ superlattices $H(LH)^n(substrate)$, made of silica (L) and titanium oxide (H), are plotted as functions of the wavelength λ. As in Fig. 2, $\tilde{\tau}_n$ has a resonant and band structure behavior. In the gaps $\tilde{\tau}_n < \tau_f$ and is larger than the single-cell tunneling time τ_1.

In the wide gap region, $\tilde{T}_n$ goes to zero and $\tilde{\tau}_n$ again approaches the STT limit $\simeq \tau_1/(1 - T)$ as n increases. In the allowed band region, a resonant STT has the free motion time τ_f as its lower bound. For $\lambda = 702$ nm a STT of 2.3 fs is predicted while the measured value is approximately 2.1 ± 0.2 fs. Transmission times for other incidence angles compare well with the measured ones [15]. At variance with the massive particle's STT, the free motion time τ_f and the single-cell transmission time $\tilde{\tau}_1$ are now constant and the number of resonances does not depend on the number of wells but on the number of layers.

Let us now consider the parameter values corresponding to the system $(air)\,(substrateL)\,(HL)^n(air)$ of Ref. [2], with incidence angle $\theta_i = 20°$. In this case, there is also a wide gap with practically the same k-component phase time and low packet distortion. The predictions, shown in Fig. 1, fall within the experimental error bars for the first four points and differ from the fifth point. This is an important difference that has to be clarified. While the predicted STT grows monotonically as a function of n towards the STT limit τ_∞, the fifth experimental point implies a reduction in the STT for larger n. If that was true, the transmission time would eventually become zero by increasing the superlattice size. I believe that new experiments have to be done in order to clarify this issue.

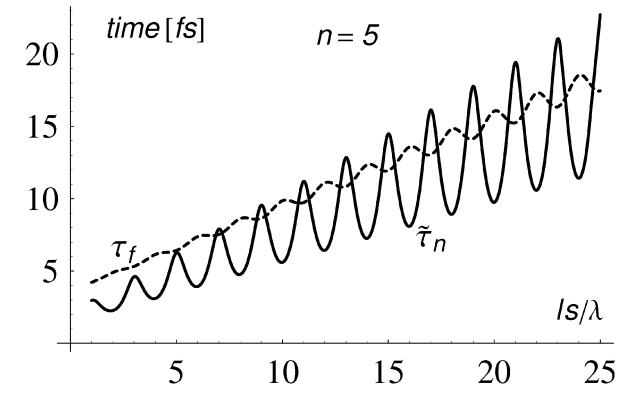

FIG. 5. To show the substrate width l_s effect on the tunneling time, we consider both a $(\lambda/4)$ superlattice $H(LH)^n(substrateL)$ with tunneling time $\tilde{\tau}_n$ and a system with tunneling time τ_f where the superlattice is replaced by air. $\lambda = 702$ ns and is kept fixed. At $4l_s/\lambda = m$ even(odd) $\tilde{\tau}_n$ reaches a minimum (maximum) and it is $< \tau_f$ $(> \tau_f)$.

In this Letter, the transfer matrix approach for finite periodic systems has been used to derive analytic and rigorous expressions for the evaluation of the superlattice-tunneling (or transmission) time τ_n and the striking STT limit $\tau_\infty \simeq \tau_1/(1 - T)$. Various experimentally observed evidences and properties of superlumina passage times through multilayer optical systems are well described. Interesting energy dependences are found. The superlattice-tunneling time τ_n exhibits a clear resonant-band structure behavior, and small times can be expected only in the gap. In the band region, the time τ_n is always larger than the free motion time τ_f, and in the gap τ_n is larger than the single-cell time τ_1. As for the wave packets, it is easy to understand the reshaping phenomena based on the k-component STT behavior. In general, wave packets with frequency components having different passage times will, obviously, be distorted when transmitted and reflected [15] . By analyzing the STT behavior one can also find low distortion conditions.

The author gratefully acknowledges the support of CONACyT of Mexico under project No. 350-E9301, the hospitality of the Physics Department, Ohio University, where part of this work was done, and H. Simanjuntak for a careful reading and comments.

[1] A. M. Steinberg, P. G. Kwiat, and R. Y. Chiao, Phys. Rev. Lett. **71**, 708 (1993).
[2] Ch. Spielmann, R. Szipöcs, A. Stingl, and F. Krausz, Phys. Rev. Lett. **73**, 2308 (1994).
[3] A. Ranfagni, D. Mugnai, P. Fabeni, and G. P. Pazzi, Appl. Phys. Lett. **58**, 774 (1991).
[4] A. Enders and G. Nimtz, J. Phys. I (France) **2**, 1693 (1992).
[5] C. R. Leavens and G. C. Aers, Phys. Rev B **39**, 1202 (1989).
[6] M. Büttiker and R. Landauer, Phys. Rev. Lett. **49**, 1739 (1982).
[7] M. Büttiker, Phys. Rev. B **27**, 6178 (1983).
[8] D. Sokolovski and L. M. Baskin, Phys. Rev A **36**, 4604 (1987).
[9] J. P. Falck and E. H. Hauge, Phys. Rev B **38**, 3287 (1988).
[10] E. H. Hauge and J. A. Støvneng, Rev. Mod. Phys. **61**, 917 (1989).
[11] R. Landauer and Th. Martin, Rev. Mod. Phys. **66**, 217 (1994).
[12] D. Bohm, *Quantum Theory* (Prentice-Hall, New York, 1951).
[13] E. P. Wigner, Phys. Rev. **98**, 145 (1955).
[14] P. Pereyra, Phys. Rev. Lett. **80**, 2677 (1998).
[15] More details will be published elsewhere.
[16] T. E. Hartmann, J. Appl. Phys. **33**, 3427 (1962).